

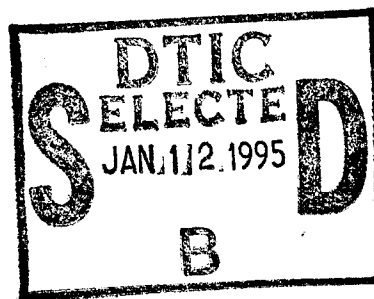
NATIONAL AIR INTELLIGENCE CENTER



NUMERICAL INVESTIGATION TO S-INLET FLOWS
(NUMERICAL SIMULATION STUDY OF S-INLET FLOWS)

by

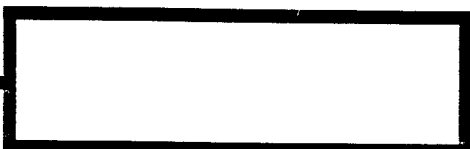
Zhang Shucheng, Huang Xijun



19950109 039

DTIC QUALITY INSPECTED 1

Approved for public release;
Distribution unlimited.



HUMAN TRANSLATION

NAIC-ID(RS)T-0922-92 17 November 1994

MICROFICHE NR: 940000492

NUMERICAL INVESTIGATION TO S-INLET FLOWS
(NUMERICAL SIMULATION STUDY OF S-INLET FLOWS)

By: Zhang Shucheng, Huang Xijun

English pages: 16

Source: Unknown; pp. 169-174

Country of origin: China

Translated by: SCITRAN
F33657-84-D-0165

Quality Control: Ruth A. Peterson

Requester: NAIC/TATV/Paul F. Freisthler

Approved for public release; Distribution unlimited.

Accession For	
NTIS GRA&I	<input checked="" type="checkbox"/>
DTIC TAB	<input type="checkbox"/>
Unannounced	<input type="checkbox"/>
Justification	
By _____	
Distribution _____	
Availability Codes	
Dist	Avail and/or Special
A-1	

THIS TRANSLATION IS A RENDITION OF THE ORIGINAL FOREIGN TEXT WITHOUT ANY ANALYTICAL OR EDITORIAL COMMENT STATEMENTS OR THEORIES ADVOCATED OR IMPLIED ARE THOSE OF THE SOURCE AND DO NOT NECESSARILY REFLECT THE POSITION OR OPINION OF THE NATIONAL AIR INTELLIGENCE CENTER.

PREPARED BY:
TRANSLATION SERVICES
NATIONAL AIR INTELLIGENCE CENTER
WPAFB, OHIO

GRAPHICS DISCLAIMER

All figures, graphics, tables, equations, etc. merged into this translation were extracted from the best quality copy available.

STOP HERE

ABSTRACT This work improves Denton's finite volume time marching methods. It takes this type of method, in which there is 1st order accuracy in time and 2d order accuracy in space, and improves it to be a calculation method in which there is 2d degree accuracy in time and 2d degree accuracy in space. In conjunction with this, application is made to numerical simulations of inlet flow fields associated with the interior flows of S type inlets as well as exterior flows which inlets possess. Calculations are carried out for actual cases, and we obtained reasonable calculation results.

KEY WORDS Inlet, Numerical Calculation, Numerical Simulation

I. FORWARD

Using time marching methods to solve original parameter equations is an effective method to make stable solutions for non-viscous, rotational flow fields. It is possible to very easily solve subsonic, transsonic, and supersonic flow fields. As far as the use of Euler equations to solve flow fields is concerned, it is only possible to carry out nonviscous numerical simulations. However, it is possible to make preliminary analyses of flow fields to a reasonable level. At the same time, Euler equation solutions are also the foundation for numerical value calculations involved with viscosity. Denton's methods^(1,2) are a type of time marching method associated with finite volumes and implicit equations of 2d order accuracy. They are primarily applied to flow field calculations for blade devices, and are a type of effective and reliable calculation form. The work in

question takes this type of method and, from 1st order accuracy in time and 2d order accuracy in space, improves it to a calculation method with 2d degree accuracy in time and 2d degree accuracy in space. In conjunction with this, it is applied to numerical simulations associated with flow fields of S inlet internal flows as well as incoming internal and external flows. It achieves reasonable results.

II. EULER EQUATIONS WHICH CONSERVE FORMS

The Euler equation set which conserves forms is

$$\frac{\partial U}{\partial t} + \frac{\partial F}{\partial x} + \frac{\partial G}{\partial y} = 0 \quad (1)$$

In this

A170

$$\begin{aligned} U &= (\rho, \rho V_x, \rho V_y, \rho e)' \\ F &= (\rho V_x, \rho V_x^2 + p, \rho V_x V_y, \rho V_x h^*)' \\ G &= (\rho V_y, \rho V_x V_y, \rho V_y^2 + p, \rho V_y h^*)' \end{aligned}$$

Corresponding status equations are:

(2)

$$\begin{aligned} h^* &= C_p T + \frac{1}{2} (V_x^2 + V_y^2) \\ e &= h^* - p / \rho \\ p &= \rho R T \end{aligned} \quad (3)$$

(4)

Taking Euler equation (1) and applying it to infinitesimal control volume ΔV , one obtains the change ΔU through time increments Δt

(5)

$$\Delta U = -\frac{\Delta t}{\Delta V} \sum_n (F dS_x + G dS_y)$$

Here $\Delta U = [\Delta p, \Delta(\rho V_x), \Delta(\rho V_y), \Delta(\rho e)]'$

From Euler equation (1), one solves steady state flow fields. With regard to uniform incoming flows, it is possible to assume that enthalpy h^* is a constant, reducing by one the required iterative equations (energy equations).

III. DENTON CALCULATION METHODS^(1,2)

As far as the use of central difference forms to solve non-stable state Euler equations is concerned, it is necessary to opt for the use of smoothing measures in order to guarantee the stability of solutions. The instability characteristics of center difference forms are clearly shown in wave motion changes associated with flow field parameter highs and lows which draw the nodal points on flow lines, that is, high speed, low pressure nodal points are consecutive. In order to resolve these problems, it is possible to opt for the use of types of head wind forms. When handling momentum equations, infinitesimal units of change ΔU (Fig.1) are directly added to nodal points down the flow. Moreover, one makes the pressures associated with nodal points down the flow be directly applied to nodal points up the flow, that is

(6)

$$p_{i,j-1}^{n+1} = p_{i,j}^n$$

$$(\rho V_x)_{i,j}^{n+1} = (\rho V_x)_{i,j}^n$$

$$+ \frac{1}{2} [\Delta (\rho V_x)_{i,j}^n + \Delta (\rho V_x)_{i-1,j}^n]$$

(7)

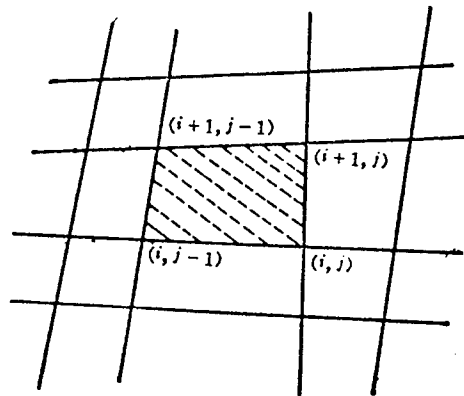


Fig.1 Infinitesimal Body

$$(\rho V_y)_{i,j}^{n+1} = (\rho V_y)_{i,j}^n$$

$$+ \frac{1}{2} [\Delta (\rho V_y)_{i,j}^n + \Delta (\rho V_y)_{i-1,j}^n]$$

(8)

This form strengthens the relationships between flow field parameters for nodal points down the flow and nodal points up the flow. By pressure restraints associated with nodal points down the flow, the speeds of nodal points up the flow are moved up or down. The accuracy is only 1st order. It is possible, with regard to the addition of corrective factor CFP values to pressure quantities, to raise the accuracy of forms.

(9)

$$p_{i,j}^{n+1} = p_{i,j}^n + CFP_{i,j}^{n+1}$$

$$CFP_{i,j}^{n+1} = (1 - RF)CFP_{i,j}^n + RF(p_{i,j+1}^n - p_{i,j}^n)$$

(10)

RF is a relaxation factor (normally, approximately equal to 0.05). At times when one reaches stable reductions or convergence restraint, the equations above become

$$p_{i,j} = p_{i,i} \quad (11)$$

As far as the forms above going through corrections in pressure quantities is concerned, this makes form accuracy become 2d order. Moreover, stability characteristics do not change. This form is called Form A.

A171

Due to the nature of flow fields, at times with low Mach numbers, changes in pressures and densities are basically consistent. Because of this, the pressure corrections in Form A are capable of changing into ones which are realized from mass equation forms, that is, density changes in infinitesimal bodies $\Delta \rho$ are applied to upper flow surfaces. One gets Form B.

$$p_{i,j-1}^{n+1} = p_{i,j-1}^n + \frac{1}{2}(\Delta \rho_{i,j}^n + \Delta \rho_{i-1,j}^n) \quad (12)$$

Others are the same as Form A.

Form B is capable of being used in low Mach number calculations existing in back flows or stagnant points. However, as far as those existing in high Mach number areas of flow fields are concerned, Form B will be unstable.

With regard to the combining of Form A and Form B, it is possible to present a type of form (Form C)

(13)

$$p_{i,j}^{n+1} = (\rho_{i,j+1}^{n+1} + CFRO_{i,j}^{n+1}) \cdot RT_{i,j}^{n+1}$$

$$CFRO_{i,j}^{n+1} = (1 - RF) \cdot CFRO_{i,j}^n + RF(\rho_{i,j}^n - \rho_{i,j+1}^n) \quad (14)$$

$$(\rho V_x)_{i,j}^{n+1} = (\rho V_x)_{i,j}^n + \frac{1}{2} [\Delta(\rho V_x)_{i,j}^n + \Delta(\rho V_x)_{i-1,j}^n]$$

$$(\rho V_y)_{i,j}^{n+1} = (\rho V_y)_{i,j}^n + \frac{1}{2} [\Delta(\rho V_y)_{i,j}^n + \Delta(\rho V_y)_{i-1,j}^n] \quad (15)$$

(16)

In this, CFRO is a density correction factor.

When one reaches a stable solution, equation (13) becomes

$$p_{i,j} = \rho_{i,j} RT_{i,j}$$

This form captures shock wave energy strengths. In conjunction with that, it is stable with regard to all Mach numbers. However, it is not capable of being applied to calculations for flow fields with reflux or back flows.

Finally, it is possible to take Form B and Form C and combine them into a unified calculation form, that is, take equation (12) and equation (13) and change them into the three equations below

(17)

$$\rho_{i,j-1}^{n+1} = \rho_{i,j}^n + \frac{1}{2} \alpha (\Delta \rho_{i,j}^n + \Delta \rho_{i-1,j}^n)$$

$$\rho_{i,j}^{n+1} = \rho_{i,j}^n + \frac{1}{2} (1 - \alpha) (\Delta \rho_{i,j}^n + \Delta \rho_{i-1,j}^n) \quad (18)$$

$$p_{i,j}^{n+1} = RT_{i,j}^{n+1} [\alpha \rho_{i,j}^{n+1} + (1 - \alpha) (\rho_{i,j+1}^{n+1} + CFRO_{i,j}^{n+1})] \quad (19)$$

In the equations, α is a distribution function.

When $Ma < 1$, $a = 1$

$Ma \geq 1$, $a = 0$

However, giving a in this way, when solving two and three dimension flow fields, one will see the appearance of continuity problems. a is capable of being defined as the temperature function

$$\alpha = 0.5 \left(1 + \frac{T - T^*}{T_0 - T^*} \right) \quad \alpha \geq 0 \quad (20)$$

In the equation, T_0 is the overall temperature. T^* is critical temperature.

Energy equations are capable of using center difference forms or processing equations of the same types as equation (17) and equation (18) with regard to continuity equations.

This form is capable of calculations in various types of flow fields with high and low Mach numbers as well as those with reflux or back flows.

Distribution function a does not influence stable solutions after convergence. It only guarantees form stability with regard to flow field calculations. When calculating shock waves, one must still introduce 2d order artificial viscosity terms in order to eliminate shock wave oscillations. Then, equation (19) becomes

$$p_{i,j}^{n+1} = RT_{i,j}^{n+1} \left(\alpha \rho_{i,j}^{n+1} + (1 - \alpha) (\rho_{i,j+1}^{n+1} + CFRO_{i,j}^{n+1}) + (\rho_{i,j-1}^{n+1} - \rho_{i,j}^{n+1}) (\rho_{i,j+1}^{n+1} - \rho_{i,j-1}^{n+1}) / \rho_{i,j}^{n+1} \right) \quad (21)$$

Denton forms, in reality, are a type of mixed difference form. In drawing up flow line directions, with regard to Euler equations, one should use reflux difference forms. In the case of all vertical directions, one should use center difference forms. The results are 1st order

A172

accuracy in time and 2d order accuracy in space. Below, corrections are carried out on solutions associated with ΔU . It is possible to make Denton calculation forms rise from 1st order accuracy in time to 2d order accuracy in time.

From equation (1), one obtains

$$\frac{\partial U}{\partial t} = -\left(\frac{\partial F}{\partial x} + \frac{\partial G}{\partial y}\right)$$

Now make

$$\delta U^{n+1} = U^{n+1} - U^n$$

Because

$$\begin{aligned} \delta U^{n+1} &= \left(\frac{\partial U}{\partial t}\right)^{n+1} \cdot \Delta t + \left(\frac{\partial^2 U}{\partial t^2}\right)^{n+1} \frac{\Delta t^2}{2} + 0(\Delta t^3) \\ &= -\frac{3}{2} \left(\frac{\partial F}{\partial x} + \frac{\partial G}{\partial y}\right)^{n+1} \Delta t + \frac{1}{2} \left(\frac{\partial F}{\partial x} + \frac{\partial G}{\partial y}\right)^n \Delta t + 0(\Delta t^3) \end{aligned}$$

The equations above then take their integrals versus infinitesimal bodies ΔV , and one obtains

$$\delta U^{n+1} = -\frac{3}{2} \Delta U^{n+1} - \frac{1}{2} \Delta U + 0(\Delta t^3) \quad (22)$$

With equation (22), one corrects $\Delta \rho$, $\Delta(\rho v_x)$, $\Delta(\rho v_y)$, and $\Delta(\rho e)$. One is then able, presupposing virtually no increase in the amount of calculations, to raise the accuracy of the forms.

When applying the equations in question to carry out numerical simulations, iterative processes associated with equations should be

(1) In solving continuity equations, to solve for new densities

(2) In solving energy equations, to obtain new internal energies

(3) Using new densities, new internal energies as well as old velocities, to calculate new pressures

(4) Using new pressures, solving momentum equations to get new speeds.

Using this sequence to treat Euler equations, one is able to guarantee optimum stability in association with the forms.

IV. STABILITY

Denton methods are time marching methods associated with implicit equations. Their time increment Δt is limited by stability conditions:

$$\Delta t \leq \frac{\Delta l}{V + a}$$

l is the grid infinitesimal flow direction width. In actual calculations, it is possible to take the above equation and simplify it to be

$$\Delta t \leq FT \cdot \frac{\Delta x}{\sqrt{KRT_0}}$$

In this, FT is the time increment. Generally, $FT = 0.1 \sim 0.5$.

In actual flow field calculations, one will also normally see the appearance, in iterative processes, of excessively large flow field parameter changes associated

with certain special points, producing non-stable state, unstable phenomena. As far as the appearance of this type of situation is concerned, if control is not added, it is possible that it will lead to iterative divergence. One effective method for resolving this problem is to introduce into the procedure feedback factors. They are only applied when there is a trend toward the appearance of instability. Reducing the corresponding grid point parameter changes restrains the development of unstable influences, guaranteeing iterative convergence

V. BOUNDARY CONDITIONS

As is shown in Fig.2, within S inlets, there are three types of boundaries all together: intake, exhaust, and wall surface or skin boundaries. In Fig.3, what is shown is S inlets possessing incoming flow exterior fields. All together, there are five types of boundaries: incoming flow, distant flow, exterior flow exhaust or exit, interior flow exhaust or exit, as well as wall surface or skin boundaries.

It is possible to know, from deductions of characteristics theory, that, when incoming flows are subsonic, incoming flow boundaries or interior flow intake boundaries should fix three flow movement parameters. Generally, they fix overall temperature T_0 , overall pressures p_0 , as well as flow movement angle. When interior flow exhausts or exits or exterior flow exhausts or exits have subsonic flows, their corresponding boundaries should fix one flow movement parameter. Generally, they fix static pressure distribution. With regard to wall surface or skin boundaries, it is possible to use mutually tangent flow movement conditions. As far as the exterior flow

A173

distant field boundaries of Fig.3 are concerned, it is only necessary for boundaries to be sufficiently distant from inlets, and it is possible to fix or designate free flow autonomous conditions.

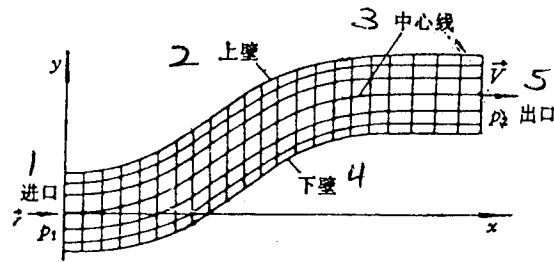


Fig.2 S Inlet Interior Flow Grid (1) Intake (2) Upper Wall (3) Lower Wall (4) Center Line (5) Exhaust or Exit

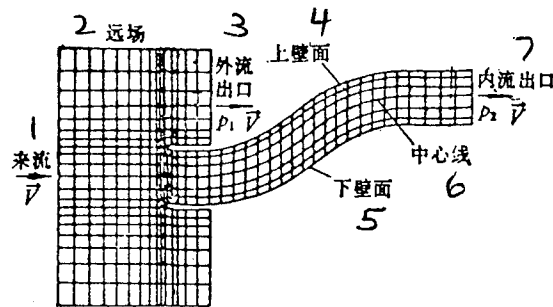


Fig.2 S Inlet Grid Possessing Exterior Flows (1) Incoming Flow (2) Distant Field (3) Exterior Flow Exhaust or Exit (4) Upper Wall Surface or Skin (5) Lower Wall Surface or Skin (6) Center Line (7) Interior Flow Exhaust or Exit

VI. INITIAL FLOW FIELDS AND GRIDS

What is capable of defining initial flow fields is:
(1) overall temperature and overall pressure along the drawn up flow lines being constant (2) static pressure along drawn up flow lines changing in a linear way, and (3) the flow direction of the entire flow field conforming to the direction of a drawn up central flow line. Numerical tests demonstrate that defining initial flow fields in this way is feasible.

As shown in Fig.2 and Fig.3, grids are composed of drawn up flow lines and vertical transversals.

VII. CALCULATED INSTANCES AND CONCLUSIONS

Fig.4(a) is a calculation grid for an interior convex channel. It is composed from 31x13 individual nodal points. Fig.4(b) is a subsonic calculation result for a channel of this geometry. Flow field intake Mach numbers are all 0.5. Symmetry characteristics for these results are good. They are basically the same as finite volume time marching method calculation results associated with N_i (unclear)⁽³⁾. Fig.4 (c) is the convergence history for this calculated instance. There were all together 1000 iterative increments. The maximum residual difference associated with x direction velocities was smaller than 1.1×10^{-5} .

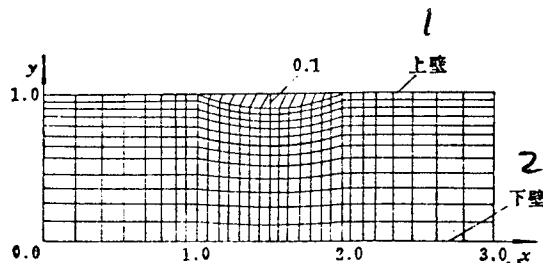


Fig.4(a) Convex Channel Calculation Grid (1) Upper Wall
(2) Lower Wall

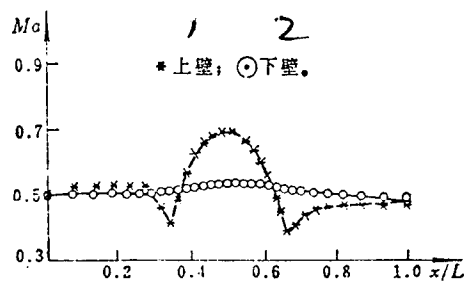


Fig.4(b) Mach Number Distributions Associated with Channel Upper and Lower Walls (1) Upper Wall (2) Lower Wall

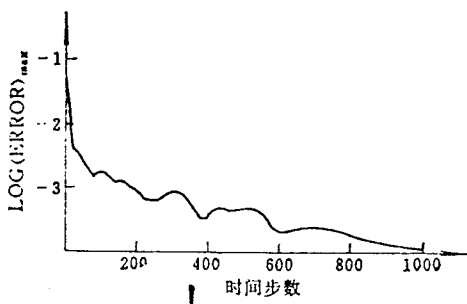


Fig.4(c) Convergence History (1) Time Increment Number

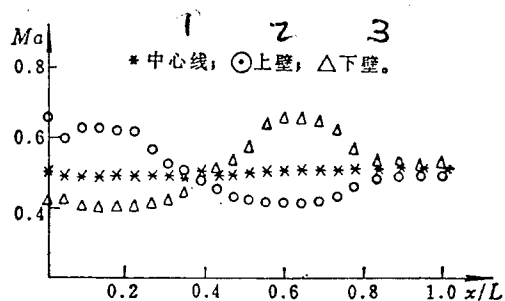


Fig.5 Mach Number Distributions Associated with Two Dimensional S Type Interior Flow Channels (1) Center Line (2) Upper Wall (3) Lower Wall

Fig.5 is calculation results for a two dimensional S type channel as shown in Fig.2. The grid points are 23x7. Boundary conditions for incoming flows are given as uniform overall pressure p_0 equal to 101330.0 Pa, uniform overall temperature T_0 of 288 K, as well as y direction velocity component V equal to zero.

Fig.6 is the results gotten from carrying out calculations after the equivalent section associated with a 10% addition in length to the Fig.2 inlet position. The boundary conditions given are the same as those for Fig.5 calculated instances. This result eliminates the pulsations in flow field distributions at intake positions in Fig.5 calculated instances. The reason is that one is given an incoming flow boundary condition of $V_y = 0$. Addition of equivalent sections makes it possible to guarantee that the realization of these conditions will be even more rational.

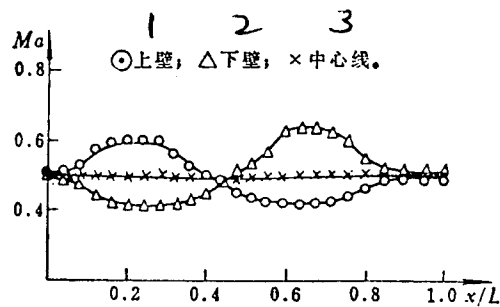


Fig.6 S Inlet Mach Number Distribution Associated with the Addition of Equivalent Sections (Not Including Exterior Flows) (1) Upper Wall (2) Lower Wall (3) Center Line

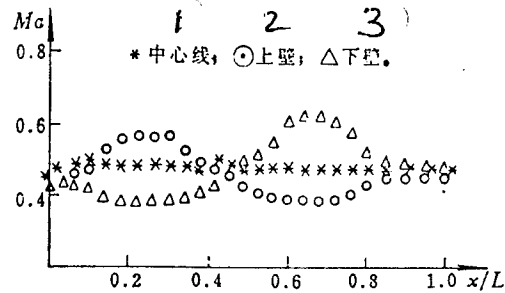


Fig.7 Mach Number Distributions Associated with S Type Inlets (1) Center Line (2) Upper Wall (3) Lower Wall

Fig.7 is calculation results for S type inlets possessing incoming flow exterior fields as shown in Fig.3. Incoming flow and interior flow exit boundary conditions are the same as those for Fig.5 calculated instances. In conjunction with this, the given distant field boundary conditions and incoming flow boundary conditions are the same. Exterior flow exhaust or exit boundary conditions are given as uniform static pressure p_1 equal to 83688.4 Pa. Results clearly show that Fig.7's Mach number distribution and Fig.6's Mach number distribution are basically consistent. This type of result is rational.

Going through several calculated instances, one comes to a number of conclusions.

(1) Denton method calculation efficiencies on IBM 4341 computers are each grid point each time increment approximately 1.0×10^{-3} s. One normally requires 500 iterative increments. Maximum residual errors associated with x direction velocity components in flow fields are all capable of being less than 0.5×10^{-3} .

(2) Convergence standards can be fixed to be maximum residual errors smaller than 0.5×10^{-3} .

(3) Euler equation processing procedures influence solution stability characteristics.

(4) Denton method numerical simulations with regard to S inlet flow fields are feasible. Using Euler equations to simulate non-viscous flow fields, it is possible to provide flow field distribution reference values.

REFERENCES

- (1) Denton J D. A Time Marching Method for Two-and-Three-Dimensional Blade to Blade flows., ARC R & M, 3775, 1975
- (2) Denton J D. An Improved Time Marching Method for Turbomachinery Flow Calculation. ASME paper, 82-GT-239, 1982
- (3) Ron-Ho Ni. A Multiple-Grid Scheme for Solving the Euler Equations. AIAA Journal. 1987, 20: (11) 1565-1571

- (4) Hobson, D.E.; "Velocity Graphing Methods Associated with Designing Transsonic Turbine Blades and Studies on High Load Transsonic Turbine Aerodynamics Designs, Calculations, and Tests"(First Collection), 1977

- (5) Lin Qi, Guo Rongwei; "In S Curved Tubes, Compressible Three Dimensional Turbulent Flow Control Equations and Calculations", ACTA AERONAUTICA ET ASTRONAUTICA SINICA, 1986, 7(2)

DISTRIBUTION LIST

DISTRIBUTION DIRECT TO RECIPIENT

<u>ORGANIZATION</u>	<u>MICROFICHE</u>
B085 DIA/RTS-2FI	1
C509 BALLOC509 BALLISTIC RES LAB	1
C510 R&T LABS/AVEADCOM	1
C513 ARRADCOM	1
C535 AVRADCOM/TSARCOM	1
C539 TRASANA	1
Q592 FSTC	4
Q619 MSIC REDSTONE	1
Q008 NTIC	1
Q043 AFMIC-IS	1
E051 HQ USAF/INET	1
E404 AEDC/DOF	1
E408 AFWL	1
E410 AFDTC/IN	1
E429 SD/IND	1
P005 DOE/ISA/DDI	1
P050 CIA/OCR/ADD/SD	2
1051 AFIT/LDE	1
PO90 NSA/CDB	1
2206 FSL	1

Microfiche Nbr: FTD94C000492
NAIC-ID(RS)T-0922-92